



Cite this: *Dalton Trans.*, 2015, 44, 5961

Received 28th November 2014,
Accepted 11th February 2015

DOI: 10.1039/c4dt03655g

www.rsc.org/dalton

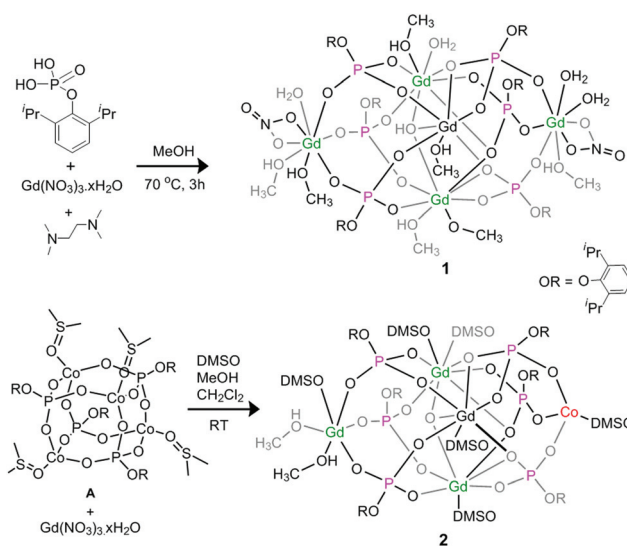
Discrete $\{\text{Gd}^{\text{III}}_4\text{M}\}$ ($\text{M} = \text{Gd}^{\text{III}}$ or Co^{II}) pentanuclear complexes: a new class of metal-organophosphate molecular coolers†

Sandeep K. Gupta,^a Aijaz A. Dar,^a Thayalan Rajeshkumar,^a
Subramaniam Kuppaswamy,^a Stuart K. Langley,^b Keith S. Murray,^b
Gopalan Rajaraman^a and Ramaswamy Murugavel*^a

The first examples of homo- and hetero-polymetallic organophosphates of gadolinium are reported. Magnetic measurements reveal a higher magnetic entropy change for the isotropic $\{\text{Gd}^{\text{III}}_5\}$ complex ($25.8 \text{ J kg}^{-1} \text{ K}^{-1}$) as compared to the heterometallic $\{\text{Gd}^{\text{III}}_4\text{Co}^{\text{II}}\}$ complex ($20.3 \text{ J kg}^{-1} \text{ K}^{-1}$), which is attributable to a change in magnetic coupling as estimated from DFT calculations.

Lanthanide coordination complexes have been widely investigated in recent times due to their interesting magnetic properties and potential technological applications such as low temperature cryogenic coolers,¹ single molecule magnets,² and quantum computing devices.³ In particular, it has been shown that many $\{3d\}$,⁴ $\{\text{Gd}^{\text{III}}\}$ ⁵ and $\{3d\text{-Gd}^{\text{III}}\}$ ⁶ complexes exhibit a significant magneto-caloric effect (MCE). Among these the most effective cooling devices are complexes containing the Gd^{III} ion,⁵ necessitating further investigations on homo- Gd^{III} and hetero-metallic $\{3d\text{-Gd}^{\text{III}}\}$ based systems with newer types of complex forming ligands, such as phosphate monoesters.⁷ Since phosphorus based ligands can mediate weak exchange coupling between isotropic ions such as Gd^{III} , organophosphonates and phosphates are ideal candidates to obtain large MCE values.⁸ Although several lanthanide organophosphonate complexes have been studied for their MCE properties,^{6a-e} to the best of our knowledge, no organophosphate based lanthanide complexes are known to date.

The reaction of 2,6-di-iso-propylphenylphosphate (dippH_2)⁹ with $\text{Gd}(\text{NO}_3)_3 \cdot 6\text{H}_2\text{O}$ in the presence of tmeda (1 : 1 : 2) in methanol yielded $[\text{Gd}^{\text{III}}_5(\mu_3\text{-OH})(\text{NO}_3)_2(\text{dipp})_6(\text{MeOH})_7(\text{H}_2\text{O})_4] \cdot 5\text{MeOH}$ (**1**) (Scheme 1). The introduction of Co^{II} inside the above pentanuclear Gd^{III} complex, **1** has been achieved *via* a different synthetic strategy, employing the preformed cobalt



Scheme 1 Synthesis of Gd_5 and Gd_4Co organophosphate complexes **1** and **2**.

phosphate $[\text{Co}(\text{dipp})(\text{DMSO})_4(\text{A})]^{10}$ complex as a combined source of the cobalt and phosphate ligand. Diffusion of a CH_2Cl_2 solution into a $\text{DMSO}\text{-MeOH}$ solution of $\text{Gd}(\text{NO}_3)_3 \cdot 6\text{H}_2\text{O}$ and **A** resulted in the isolation of single crystals of $[\text{Gd}^{\text{III}}_4\text{Co}^{\text{II}}(\mu_3\text{-O})(\text{dipp})_6(\text{DMSO})_6(\text{MeOH})_2] \cdot \text{H}_2\text{O}$ (**2**), through scrambling (Scheme 1).

Solid state molecular structures of **1** and **2** were determined by single crystal X-ray diffraction studies (Fig. 1). The cores of both **1** and **2** are pentanuclear $\{\text{M}_5(\text{dipp})_6\}$ units, built around either a triply-bridging $\mu_3\text{-OH}^-$ (for **1**) or $\mu_3\text{-O}^{2-}$ (for **2**) ligand, resembling the structure of pentanuclear Ti^{IV} and Fe^{III} complexes recently reported by us.¹¹ While $\mu_3\text{-OH}$ or $\mu_3\text{-O}$ bridged metal-triangular complexes are commonly formed when bridging RCO_2^- carboxylate ligands are employed, due to the presence of an extra oxygen atom and negative charge, organophosphates $((\text{RO})\text{PO}_3)^{2-}$ have the ability to embrace two more metal ions and form pentanuclear complexes, as shown in Scheme S1 (ESI†). For example, the $\mu_3\text{-OH}^-$ and six dipp^{2-}

^aDepartment of Chemistry, Indian Institute of Technology Bombay, Powai, Mumbai, Maharashtra 400076, India. E-mail: rmv@chem.iitb.ac.in

^bSchool of Chemistry, Monash University, Clayton, Victoria 3800, Australia

† Electronic supplementary information (ESI) available: Experimental and computational details as a PDF; CIF for **1** (CCDC 1030609) and **2** (CCDC 1030610). CCDC 1030609 and 1030610. For ESI and crystallographic data in CIF or other electronic format see DOI: 10.1039/c4dt03655g

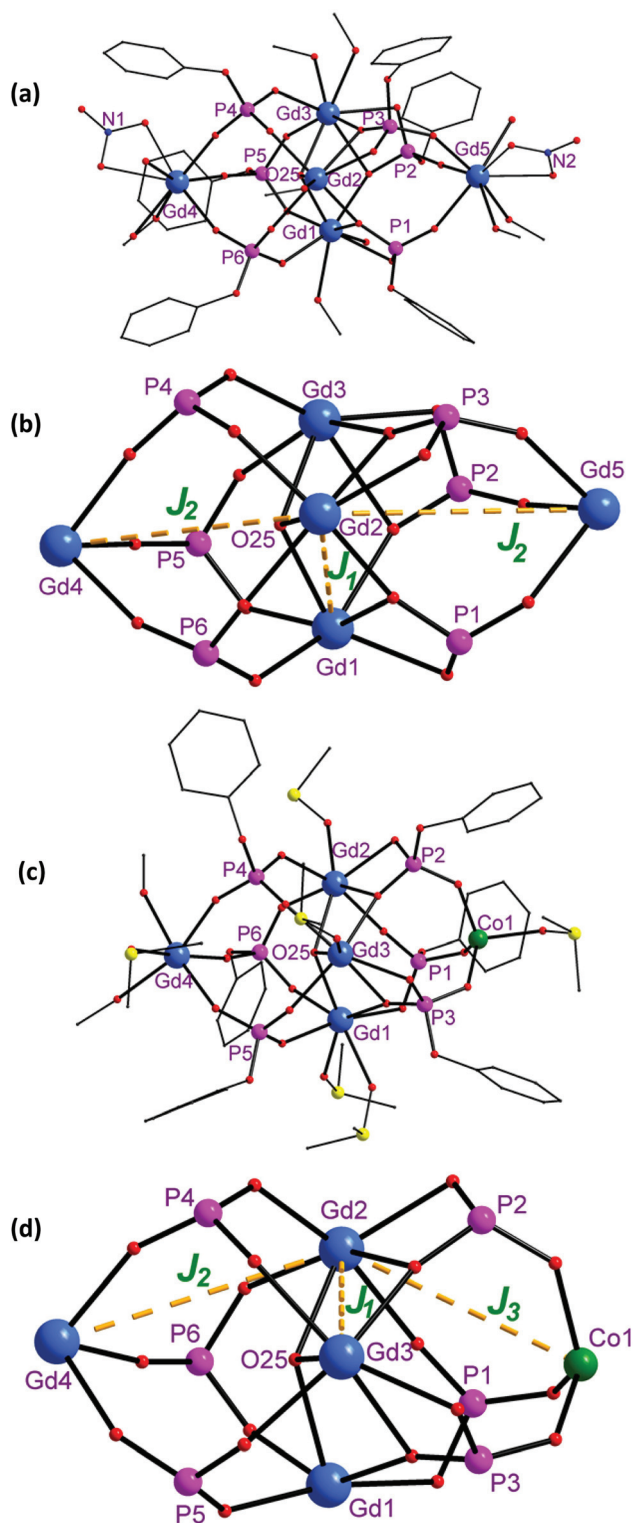


Fig. 1 (a & b) Molecular and core structure of **1**; (c & d) molecular and core structure of **2**. Lattice solvent molecules, isopropyl groups and H-atoms are omitted for clarity. Dotted lines indicate the different magnetic exchange interaction pathways.

ligands in **1** form the $[\text{Gd}_3(\mu_3\text{-OH})(\text{dipp})_6]$ trinuclear unit, utilizing two of the phosphate oxygen atoms. A third oxygen atom of the six dangling phosphate ligands then binds to two different Gd^{III} ions on either side of the triangular complex to complete the pentanuclear motif. The coordination unsaturation and charge balance is then taken care of by peripheral nitrate, water, and methanol ligands. The structure of **2** is very similar to **1**, the difference being the substitution of a divalent cobalt ion in place of a trivalent Gd ion and an oxo ligand replacing a hydroxo group at the centre of the complex. Since the charge balance has been achieved from phosphate and oxo ligands, there are no nitrates found in **2**. The phosphate ligands in **1** and **2** on the left side of the complexes exhibit the $[3.111]$ mode of coordination (Harris notation¹²), while those on the right side exhibit the $[3.211]$ mode of coordination (Scheme 1 and Fig. 1).

The distances between the Gd^{III} ions in the central triangle, $\text{Gd1}\cdots\text{Gd2}$, $\text{Gd2}\cdots\text{Gd3}$ and $\text{Gd1}\cdots\text{Gd3}$ in **1** are 3.8865(8), 3.9399(9), and 3.9192(8) Å, respectively, with the central hydroxo oxygen lying 0.893 Å above the triangle. The eight-coordinate Gd1 , Gd3 , Gd4 , and Gd5 ions exhibit distorted triangular dodecahedral geometries, whereas the seven-coordinate Gd2 ion adopts a distorted pentagonal bipyramidal geometry.¹³ The distance between the two terminal, Gd4 and Gd5 ions is 10.149(2) Å. The $\text{Gd1}\cdots\text{Gd2}$, $\text{Gd2}\cdots\text{Gd3}$ and $\text{Gd1}\cdots\text{Gd3}$ metal–metal distances in the central triangular unit of **2** are 4.140(1), 3.888(1) and 3.903(1) Å, respectively, with the central oxo ligand lying 0.736 Å above the metal triangle. The distances of the tetrahedral Co1 ion from Gd1 , Gd2 and Gd3 are 4.944(1), 4.739(1) and 4.838(8) Å, respectively, whereas the distance to the terminal Gd4 ion is 9.17(2) Å. The central seven-coordinate Gd1 , Gd2 and Gd3 ions adopt distorted pentagonal bipyramidal geometries, while the terminal Gd4 ion exhibits a distorted octahedral geometry.

Variable temperature direct current (dc) magnetic susceptibility measurements were performed for complexes **1** and **2** between 2 and 300 K under an applied field of 1.0 T (Fig. 2). The $\chi_{\text{M}}T$ value of 39.58 $\text{cm}^3 \text{K mol}^{-1}$ at 300 K for **1** is in good agreement with the calculated value of 39.40 $\text{cm}^3 \text{K mol}^{-1}$ ($g = 2$) for five non-interacting Gd^{III} ions. The $\chi_{\text{M}}T$ value for **2** at ~ 300 K is 33.17 $\text{cm}^3 \text{K mol}^{-1}$ similar to the value expected for non-interacting four Gd^{III} and one Co^{II} ions. For complex **1**, as the temperature is reduced, the $\chi_{\text{M}}T$ product remains almost constant reaching 37.71 $\text{cm}^3 \text{K mol}^{-1}$ at 8.7 K, with complex **2** displaying similar behaviour, reaching 30.7 $\text{cm}^3 \text{K mol}^{-1}$ at 8.7 K. Below 8.7 K the $\chi_{\text{M}}T$ value decreases drastically reaching 26.40 $\text{cm}^3 \text{K mol}^{-1}$ for **1** and 20.87 $\text{cm}^3 \text{K mol}^{-1}$ for **2** and suggests the presence of weak antiferromagnetic interactions. Magnetization measurements reveal the magnetization value saturates for **1** and **2** in an applied field of 7 T at 2 K, reaching a value of 34.9 and 30.12 μ_{B} , respectively. These values approach closely to that expected for five non-interacting Gd^{III} ions for **1** and four non-interacting Gd^{III} ions and a Co^{II} ion for **2**.

The magnetic data of **1** and **2** were fitted using PHI software¹⁴ employing the following exchange interactions for **1**

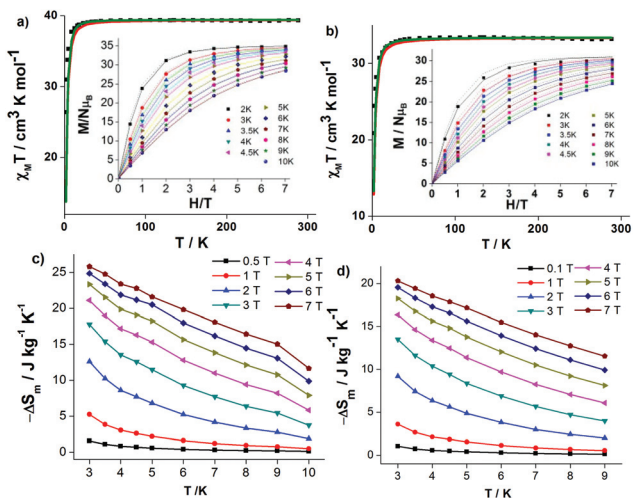


Fig. 2 (a & b) Temperature dependence of $\chi_M T$ under an applied field of 1.0 T for **1** and **2** respectively (black squares – experimental points; red line – fit; green line – DFT simulated). Insets are corresponding magnetization plots for **1** and **2** [black squares – experimental points; solid lines – fit; dotted lines – DFT simulated, see ESI† for enlarged plots]. (c) $-\Delta S_m$ values calculated from magnetization data of **1** at different temperatures and fields. (d) $-\Delta S_m$ values calculated from magnetization data of **2** at different temperatures and fields.

and **2**, respectively (zero field splitting is assumed to be zero; see below the rationale for the use of two and three different exchange constants for **1** and **2**, respectively).

$$\begin{aligned} \hat{H}_{\text{Ex}} = & -J_1(\hat{S}_{\text{Gd1}} \cdot \hat{S}_{\text{Gd2}} + \hat{S}_{\text{Gd2}} \cdot \hat{S}_{\text{Gd3}} + \hat{S}_{\text{Gd1}} \cdot \hat{S}_{\text{Gd3}}) \\ & -J_2(\hat{S}_{\text{Gd1}} \cdot \hat{S}_{\text{Gd4}} + \hat{S}_{\text{Gd2}} \cdot \hat{S}_{\text{Gd4}} + \hat{S}_{\text{Gd3}} \cdot \hat{S}_{\text{Gd4}} \\ & + \hat{S}_{\text{Gd1}} \cdot \hat{S}_{\text{Gd5}} + \hat{S}_{\text{Gd2}} \cdot \hat{S}_{\text{Gd5}} + \hat{S}_{\text{Gd3}} \cdot \hat{S}_{\text{Gd5}}) \end{aligned} \quad (1)$$

$$\begin{aligned} \hat{H}_{\text{Ex}} = & -J_1(\hat{S}_{\text{Gd1}} \cdot \hat{S}_{\text{Gd2}} + \hat{S}_{\text{Gd2}} \cdot \hat{S}_{\text{Gd3}} + \hat{S}_{\text{Gd1}} \cdot \hat{S}_{\text{Gd3}}) \\ & -J_2(\hat{S}_{\text{Gd1}} \cdot \hat{S}_{\text{Gd4}} + \hat{S}_{\text{Gd2}} \cdot \hat{S}_{\text{Gd4}} + \hat{S}_{\text{Gd3}} \cdot \hat{S}_{\text{Gd4}} \\ & -J_3(\hat{S}_{\text{Gd1}} \cdot \hat{S}_{\text{Co1}} + \hat{S}_{\text{Gd2}} \cdot \hat{S}_{\text{Co1}} + \hat{S}_{\text{Gd3}} \cdot \hat{S}_{\text{Co1}}) \end{aligned} \quad (2)$$

The best fit parameters obtained for complex **1** are $J_1 = -0.011 \text{ cm}^{-1}$ and $J_2 = -0.001 \text{ cm}^{-1}$ (spin ground state, $S = 13/2$) and in the case of **2**: $J_1 = -0.0023 \text{ cm}^{-1}$, $J_2 = -0.0092 \text{ cm}^{-1}$ and $J_3 = -0.0755 \text{ cm}^{-1}$ (Fig. 2) (spin ground state, $S = 11/2$). As Gd^{III} containing complexes are of major interest in understanding and developing the MCE in molecular coordination complexes, the entropy change has been evaluated for **1** and **2** from the magnetization data using the Maxwell relationship:

$$\Delta S_m(T)_{\Delta B} = \int \left[\frac{\partial M(T, B)}{\partial T} \right]_B dB \quad (\text{see Fig. 2(c) and (d)}).$$

The maximum theoretical entropy values are evaluated as 29.6 and 27 $\text{J kg}^{-1} \text{K}^{-1}$ for **1** and **2** (at 3 K and 7 T), respectively, using the relationship $S_m = nR \ln(2S + 1)$. The experimentally determined maximum changes in magnetic entropy are found to be 25.8 and 20.3 $\text{J kg}^{-1} \text{K}^{-1}$ for **1** and **2**, respectively for a field change of 7 T at 3 K. These $-\Delta S_m$ values are significant for the first generation Gd-phosphates, although much larger values have been found for other gadolinium systems.⁵ⁱ Despite the very small J values, there is a significant reduction on the MCE

values, particularly so in the case of **2**. To probe this observation/effect further, we have evaluated the exchange interaction pathways in both **1** and **2** using DFT calculations (see ESI†). The calculations have been performed starting from the crystal structures of **1** and **2**.

In complex **1** two exchange interactions are modelled. The first is between the Gd^{III} ions within the gadolinium triangular unit, Gd1–Gd3, present at the centre of the complex (see Fig. 1) (J_1). The second interaction J_2 describes the interaction between the central triangular Gd^{III} ions with the terminal Gd^{III} ions, Gd4 and Gd5 (Fig. 1). In the case of complex **2**, the J_1 and J_2 interactions are similar to that in complex **1** and, in addition to these interactions, the exchange between Co^{II} and Gd^{III} ions is treated as J_3 . The DFT computed exchange interactions for **1** are $J_1 = -0.0013 \text{ cm}^{-1}$, $J_2 = 0.0001 \text{ cm}^{-1}$ and for **2** $J_1 = -0.0502 \text{ cm}^{-1}$, $J_2 = 0.0001 \text{ cm}^{-1}$, and $J_3 = -0.0159 \text{ cm}^{-1}$. The magnetic data have been simulated using the DFT computed J values (PHI software) and there is a striking match between the experimental data and the DFT simulated curve offering confidence on the computed J parameters (see Fig. 2). Minor deviations are however found compared to J values obtained by fitting the experimental data. Since the J s are extremely small (both experimental and DFT), multiple solutions are possible for fitting the featureless curves.

The J_1 interaction mediates *via* the $\mu_3\text{-O(H)}$ and the phosphate bridges in **1** and the $\mu_3\text{-O}$ and the phosphate bridges in **2**. This interaction is found to be antiferromagnetic in both **1** and **2**. From our earlier studies on acetate bridged binuclear {Gd^{III}–Gd^{III}} complexes, the Gd–O–Gd angle was demonstrated to be an important parameter in controlling the nature of the exchange interaction.¹⁵ Here the average Gd–O–Gd angles for **1** and **2** are 108.8° and 110.9°, respectively. From these angles the exchange is therefore predicted to be very weak, at the boundary of the crossover from ferro-to-antiferro-magnetic coupling. This therefore supports the small J value calculated *via* DFT. The J_2 interaction is found to be weakly ferromagnetic and is rationalized using a spin polarization model.¹⁶

The $-\Delta S_m$ values for **1** and **2** were then calculated from the DFT J values and are found to be 26.9 and 23.9 $\text{J kg}^{-1} \text{K}^{-1}$, which are in fair agreement with the experimentally obtained $-\Delta S_m$ values. The combination of weak antiferro/ferro exchange interactions results in spin frustration within the system which brings the excited states closer to the ground state, resulting in large MCE values for **1** and **2**. The computed J_3 interaction between the Co^{II} and Gd^{III} ions in **2** is stronger than the J_2 interaction. The stronger exchange along with magnetic anisotropy associated with Co(II)¹⁷ therefore lowers the MCE values compared to **1** (see ESI†).

The computed spin density plots of the high spin states for **1** and **2** are shown in Fig. 3. The larger spin density value on the Gd^{III} ions (7.03) and lower spin density value on the Co^{II} ions (2.73) than the expected values suggest spin polarization and spin delocalization mechanisms around the respective ions. The mechanism operating in **1** and **2** can be understood from the negative spin densities on the atoms attached to the Gd^{III} ions and positive spin densities on the atoms attached to

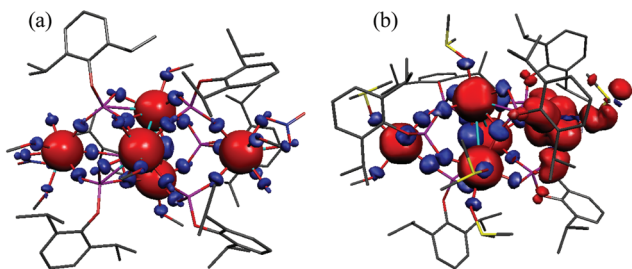


Fig. 3 Computed High Spin (HS)-density plots for (a) 1 and (b) 2. Red and blue represent positive and negative spin densities, respectively.

Co^{II} ions (Fig. 3). To further understand the effect of different transition metal ions, a simple dimeric model is constructed out of 2 (see ESI†) and the exchange interaction (J_3) is computed in which the sign (-0.037 cm^{-1}) is reproducible. As the antiferromagnetic interaction between the Co–Gd ions is found to reduce the $-\Delta S_m$ value, the role of other first transition metal ions was probed using 2 as a model by replacing Co^{II} by Mn^{II}, Fe^{II}, Ni^{II}, and Cu^{II}. The computed J values for these models are -0.027 , -0.035 , -0.003 , and -0.079 cm^{-1} for Mn^{II}, Fe^{II}, Ni^{II} and Cu^{II}, respectively. The Ni^{II} ion mediates the weakest exchange followed by the Mn^{II} ion. Since the Ni^{II} ion is likely to possess significant anisotropy, the isotropic Mn^{II} is therefore likely to be the best candidate to enhance the entropy change compared to the Co^{II} analogue.

In conclusion, we have synthesized a novel pentanuclear organophosphate complex of Gd^{III} using a phosphate monoester and a structurally similar 3d–4f analogue with Co^{II}, which are the first examples of organophosphate complexes of any lanthanide ion. The {Gd^{III}₅} complex reveals a significant entropy change ($-\Delta S_m$) of $25.8 \text{ J kg}^{-1} \text{ K}^{-1}$, at $\Delta H = 7 \text{ T}$. The high $-\Delta S_m$ values show that the organophosphate ligand based gadolinium complex displays promising MCE properties for cryogenic applications. As the maximum $-\Delta S_m$ value ($\Delta H = 7 \text{ T}$) of the {Gd^{III}₅} complex is close to the maximum attainable value, the replacement of the bulky aryl phosphate ligand with lower molecular weight phosphate ligands would enhance the entropy change ($-\Delta S_m$). Work in this direction is currently underway, apart from incorporating other 3d metal ions.

Acknowledgements

RM and GR thank the DST Nanomission (SR/NM/NS-1119/2011) and RM the DAE (2010/21/04-BRNS/2002) for financial support; SKG and AAD thank the UGC and TR the CSIR for research fellowships. KSM thanks the ARC for a Discovery grant and KSM and GR acknowledge receipt of an AISRF Australia–India science and technology grant.

Notes and references

- 1 (a) M. Evangelisti and E. K. Brechin, *Dalton Trans.*, 2010, **39**, 4672; (b) M. Evangelisti, F. Luis, L. J. de Jongh and

- M. Affronte, *J. Mater. Chem.*, 2006, **16**, 2534; (c) Y.-Z. Zheng, G.-J. Zhou, Z. Zheng and R. E. P. Winpenny, *Chem. Soc. Rev.*, 2014, **43**, 1462.
- 2 D. N. Woodruff, R. E. P. Winpenny and R. A. Layfield, *Chem. Rev.*, 2013, **113**, 5110.
- 3 T. D. Ladd, F. Jelezko, R. Laflamme, Y. Nakamura, C. Monroe and J. L. O'Brien, *Nature*, 2010, **464**, 45.
- 4 (a) M. Evangelisti, A. Candini, A. Ghirri, M. Affronte, E. K. Brechin and E. J. L. McInnes, *Appl. Phys. Lett.*, 2005, **87**, 072504; (b) R. Shaw, R. H. Laye, L. F. Jones, D. M. Low, C. Talbot-Eckelaers, Q. Wei, C. J. Milios, S. Teat, M. Helliwell, J. Raftery, M. Evangelisti, M. Affronte, D. Collison, E. K. Brechin and E. J. L. McInnes, *Inorg. Chem.*, 2007, **46**, 4968; (c) M. Manoli, R. D. L. Johnstone, S. Parsons, M. Murrie, M. Affronte, M. Evangelisti and E. K. Brechin, *Angew. Chem., Int. Ed.*, 2007, **46**, 4456; (d) M. Manoli, A. Collins, S. Parsons, A. Candini, M. Evangelisti and E. K. Brechin, *J. Am. Chem. Soc.*, 2008, **130**, 11129.
- 5 (a) F.-S. Guo, J.-D. Leng, J.-L. Liu, Z.-S. Meng and M.-L. Tong, *Inorg. Chem.*, 2011, **51**, 405; (b) F.-S. Guo, J.-D. Leng, J.-L. Liu, Z.-S. Meng and M.-L. Tong, *Inorg. Chem.*, 2011, **51**, 405; (c) G. Lorusso, M. A. Palacios, G. S. Nichol, E. K. Brechin, O. Roubeau and M. Evangelisti, *Chem. Commun.*, 2012, **48**, 7592; (d) M. Evangelisti, O. Roubeau, E. Palacios, A. Camón, T. N. Hooper, E. K. Brechin and J. J. Alonso, *Angew. Chem., Int. Ed.*, 2011, **123**, 6736; (e) S.-J. Liu, J.-P. Zhao, J. Tao, J.-M. Jia, S.-D. Han, Y. Li, Y.-C. Chen and X.-H. Bu, *Inorg. Chem.*, 2013, **52**, 9163; (f) F.-S. Guo, Y.-C. Chen, J.-L. Liu, J.-D. Leng, Z.-S. Meng, P. Vrabel, M. Orendac and M.-L. Tong, *Chem. Commun.*, 2012, **48**, 12219; (g) L.-X. Chang, G. Xiong, L. Wang, P. Cheng and B. Zhao, *Chem. Commun.*, 2013, **49**, 1055; (h) K. H. Zangana, E. M. Pineda, J. Schnack and R. E. P. Winpenny, *Dalton Trans.*, 2013, **42**, 14045; (i) G. Lorusso, J. W. Sharples, E. Palacios, O. Roubeau, E. K. Brechin, R. Sessoli, A. Rossin, F. Tuna, E. J. L. McInnes, D. Collison and M. Evangelisti, *Adv. Mater.*, 2013, **25**, 4653.
- 6 (a) Y.-Z. Zheng, M. Evangelisti and R. E. P. Winpenny, *Chem. Sci.*, 2011, **2**, 99; (b) Y.-Z. Zheng, M. Evangelisti and R. E. P. Winpenny, *Angew. Chem., Int. Ed.*, 2011, **50**, 3692; (c) E. Moreno Pineda, F. Tuna, R. G. Pritchard, A. C. Regan, R. E. P. Winpenny and E. J. L. McInnes, *Chem. Commun.*, 2013, **49**, 3522; (d) Y.-Z. Zheng, M. Evangelisti, F. Tuna and R. E. P. Winpenny, *J. Am. Chem. Soc.*, 2012, **134**, 1057; (e) Y.-Z. Zheng, E. M. Pineda, M. Helliwell and R. E. P. Winpenny, *Chem. – Eur. J.*, 2012, **18**, 4161; (f) J.-B. Peng, Q.-C. Zhang, X.-J. Kong, Y.-P. Ren, L.-S. Long, R.-B. Huang, L.-S. Zheng and Z. Zheng, *Angew. Chem., Int. Ed.*, 2011, **50**, 10649; (g) J.-B. Peng, Q.-C. Zhang, X.-J. Kong, Y.-Z. Zheng, Y.-P. Ren, L.-S. Long, R.-B. Huang, L.-S. Zheng and Z. Zheng, *J. Am. Chem. Soc.*, 2012, **134**, 3314; (h) S. K. Langley, N. F. Chilton, B. Moubaraki, T. Hooper, E. K. Brechin, M. Evangelisti and K. S. Murray, *Chem. Sci.*, 2011, **2**, 1166.

- 7 (a) R. Murugavel, S. Kuppaswamy, R. Boomishankar and A. Steiner, *Angew. Chem., Int. Ed.*, 2006, **45**, 5536; (b) R. Murugavel and S. Kuppaswamy, *Angew. Chem., Int. Ed.*, 2006, **45**, 7022; (c) R. Murugavel, S. Kuppaswamy, N. Gogoi, R. Boomishankar and A. Steiner, *Chem. – Eur. J.*, 2010, **16**, 994; (d) R. Murugavel, A. Choudhury, M. G. Walawalkar, R. Pothiraja and C. N. R. Rao, *Chem. Rev.*, 2008, **108**, 3549; (e) A. C. Kalita and R. Murugavel, *Inorg. Chem.*, 2014, **53**, 3345; (f) A. C. Kalita, N. Gogoi, R. Jangir, S. Kuppaswamy, M. G. Walawalkar and R. Murugavel, *Inorg. Chem.*, 2014, **53**, 8959; (g) H. S. Ahn and T. D. Tilley, *Adv. Funct. Mater.*, 2013, **23**, 227.
- 8 E. I. Tolis, L. P. Engelhardt, P. V. Mason, G. Rajaraman, K. Kindo, M. Luban, A. Matsuo, H. Nojiri, J. Raftery, C. Scroder, G. A. Timco, F. Tuna, W. Wernsdorfer and R. E. P. Winpenny, *Chem. – Eur. J.*, 2006, **12**, 8961.
- 9 G. M. Kosolapoff, C. K. Arpke, R. W. Lamb and H. Reich, *J. Chem. Soc. C*, 1968, **7**, 815.
- 10 [Co(dipp)(DMSO)]₄ was synthesized from cobalt(II) acetate tetrahydrate and dippH₂ in DMSO by following a similar synthetic protocol reported earlier for the preparation of the zinc analogue.^{7f}
- 11 (a) R. Murugavel and S. Kuppaswamy, *Inorg. Chem.*, 2008, **47**, 7686; (b) R. Murugavel, N. Gogoi, K. G. Suresh, S. Layek and H. C. Verma, *Chem. – Asian J.*, 2009, **4**, 923.
- 12 R. A. Coxall, S. G. Harris, D. K. Henderson, S. Parsons, P. A. Tasker and R. E. P. Winpenny, *J. Chem. Soc., Dalton Trans.*, 2000, 2349.
- 13 S. J. Lippard and B. J. Russ, *Inorg. Chem.*, 1968, **7**, 1686.
- 14 N. F. Chilton, R. P. Anderson, L. D. Turner, A. Soncini and K. S. Murray, *J. Comput. Chem.*, 2013, **34**, 1164.
- 15 (a) T. Rajeshkumar, S. K. Singh and G. Rajaraman, *Polyhedron*, 2013, **52**, 1299; (b) L. Canadillas-Delgado, J. Cano, O. Fabelo and C. Ruiz-Perez, *Gadolinium Compound: Production and Applications*, Nova Publisher, 2010.
- 16 C. Kollmar and O. Kahn, *J. Chem. Phys.*, 1992, **96**, 2988.
- 17 (a) W. Huang, T. Liu, D. Wu, J. Cheng, Z. W. Ouyang and C. Duan, *Dalton Trans.*, 2013, **42**, 15326; (b) M. R. Saber and K. R. Dunbar, *Chem. Commun.*, 2014, **50**, 12266; (c) J. Vallejo, I. Castro, R. Ruiz-Garcia, J. Cano, M. Julve, F. Lloret, G. De Munno, W. Wernsdorfer and E. Pardo, *J. Am. Chem. Soc.*, 2012, **134**, 15704; (d) F. Yang, Q. Zhou, Y. Zhang, G. Zeng, G. Li, Z. Shi, B. Wang and S. Feng, *Chem. Commun.*, 2013, **49**, 5289; (e) J. M. Zadrozny, J. Liu, N. A. Piro, C. J. Chang, S. Hill and J. R. Long, *Chem. Commun.*, 2012, **48**, 3927.